

Supporting information for...

**Lowest Aqueous Picomolar Fluoride Ion Detection by an Aluminum(III) Bind
Chemosensor and *in vivo* Aluminum-Toxicity**

Monojit Das,^{‡a} Debdeep Maity,^{‡a} Tusar Kanta Acharya,^b Sudip Sau,^a Chandan Giri,^a Chandan Goswami,^{*b} and Prasenjit Mal^{*a}

^aSchool of Chemical Sciences, National Institute of Science Education and Research (NISER), HBNI, Bhubaneswar, PO Bhipur-Padanpur, Via Jatni, District Khurda, Odisha 752050, India

^bSchool of Biological Sciences, National Institute of Science Education and Research (NISER), HBNI, Bhubaneswar, PO Bhipur-Padanpur, Via Jatni, District Khurda, Odisha 752050, India

Corresponding Author: pmal@niser.ac.in (PM); chandan@niser.ac.in (C. Goswami)

The generation of new band at 360 nm instead of 302 nm was observed in presence of 10 equiv Cu(II), Ni(II), Zn(II), Co(II). Similarly, generation of weak and broad bands were detected at 425 nm in presence of 10 equiv Cr(III) and at 375 nm for 10 equiv of Mn(II), Cd(II), Ca(II), Cr(III) etc.

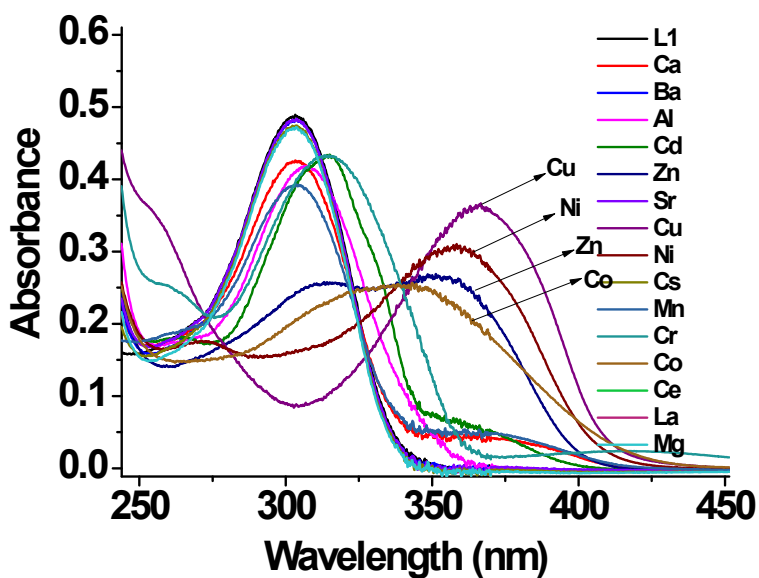


Figure S1. Absorption spectra of L1 (2×10^{-4} M) in water in presence of different cations (10 equivalent) is shown.

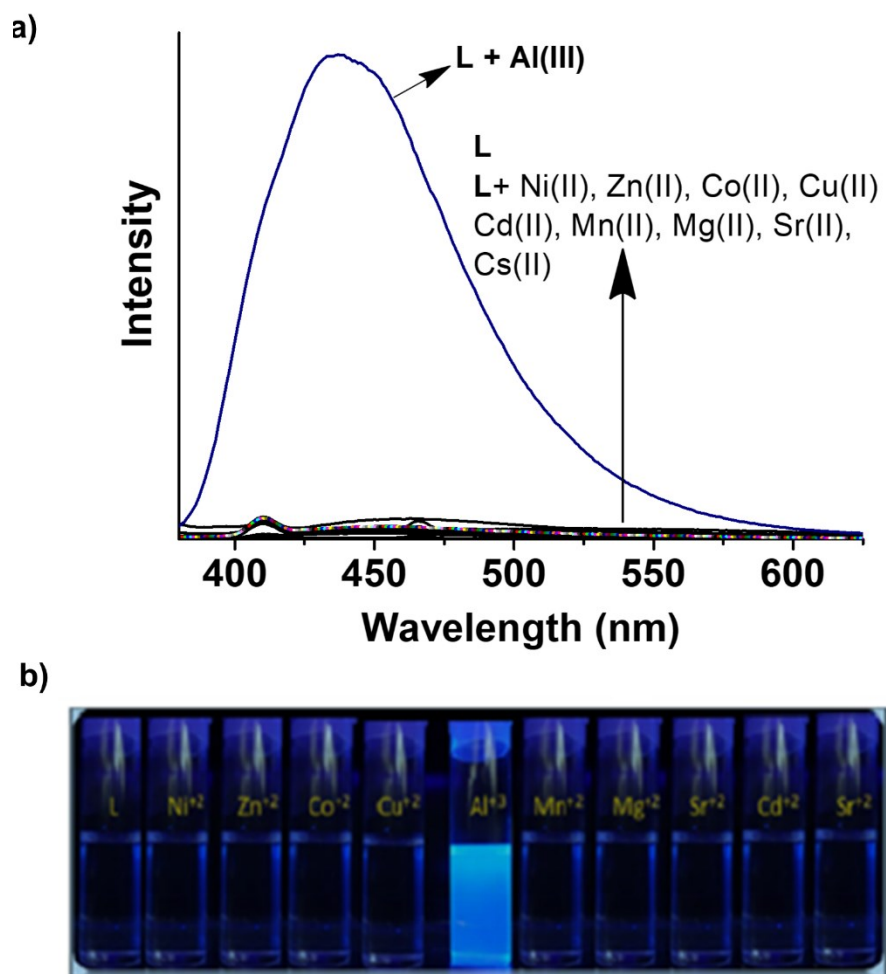


Figure S2. a) Fluorescence spectra of **L1** (2×10^{-4} M) and in the presence of different cations (2×10^{-4} M), 10 equiv each and b) Corresponding colour changes upon addition of different metal ions in water.

For UV-Vis and fluorescence titration, the same stock solutions of **L1** were used and the solutions of the nitrate salts of the Al(III) with desired concentration (0.1 - 20 equiv) were prepared by proper dilution of the stock solution. Then 2 mL of each solution was mixed in a 5 mL volumetric flask to prepare reaction mixture with 0.1 to 20-fold molar equiv of the concentration of metal ion with respect to the concentration of compounds and the absorption / fluorescence spectra of the resulting

solutions were recorded. Binding constants was calculated from fluorescence titration by following a reported procedure ¹. The interference from other metal ions was also ascertained by recording fluorescence spectra of **L1** (2×10^{-4} M) upon addition of a mixture of metal ions containing molar equiv of Al(III) and molar equiv of other metal ions with respect to the concentration of the compounds.

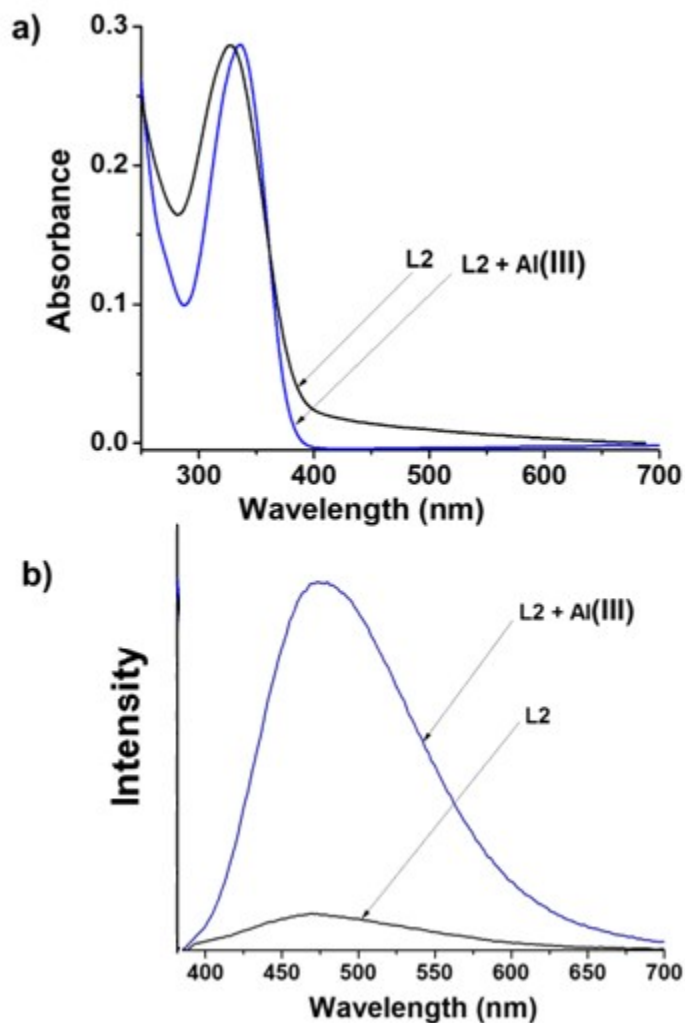


Figure S3. a) UV-Vis and b) fluorescence spectral change of **L2** in presence and absence of Al(III).

¹H NMR Analysis. ¹H NMR titration experiments helped to understand the complexation between Al(III) and ligand **L1** in a better way. In DMSO-*d*₆ spectra were recorded with increasing

concentration of Al(III) (from 0.5 equiv to 10 equiv) to the **L1**. There is very little beat change around 0.03 ppm in NMR signal of amide proton and other aryl protons and protons of pyridine ring did not show any downfield or upfield shift (Figure S4). So, it is emphasized that amide –NH and pyridyl nitrogen did not involve in the coordination with Al(III) and new signal appeared at 9.24 ppm was generated due to water coordination with Al(III) which has been disappeared after shaking with D₂O. To confirm the non-participation of nitrogen of pyridine ring in the complexation, a control experiment has been performed. Another ligand (**L2**) was synthesized by replacing pyridyl ring with a naphthalene moiety. The same change in fluorescence and UV-Vis spectra has been observed with 10 equiv. Al(III) in water (Figure S3). However, there is no significant change has been observed in the NMR signal in the presence and absence of Al(III) (Figure S5). This signifies pyridine is excluded from coordination with Al(III) but the restriction of rotation of pyridine during complexation is responsible of enhancement of fluorescence spectra of both ligand. The ¹H NMR signals at 8.65, 8.05 ppm (doublets) and two triplets at 7.95, 7.48 ppm are possibly originated from pyridine ring and three singlet at 8.55, 8.49, 8.43 ppm for the sulfonated aromatic ring and –CH=N proton. A broad singlet at 12.45 ppm indicates the presence of amide protons.

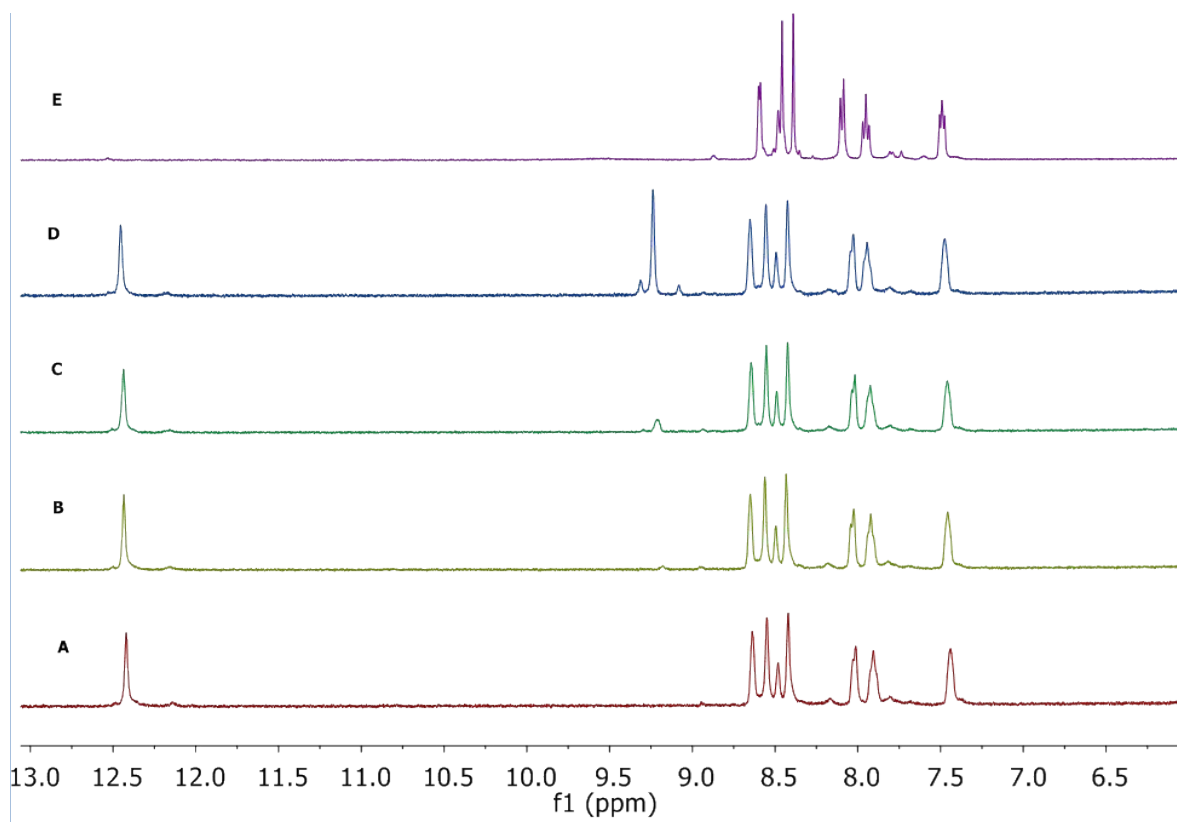


Figure S4. Partial ^1H NMR spectra in DMSO-d_6 of **L1** with addition of Al(III)A) 0 equiv B) 0.5 equiv C) 2.0 equiv D) 10.0 equiv and E) After addition of excess D_2O .

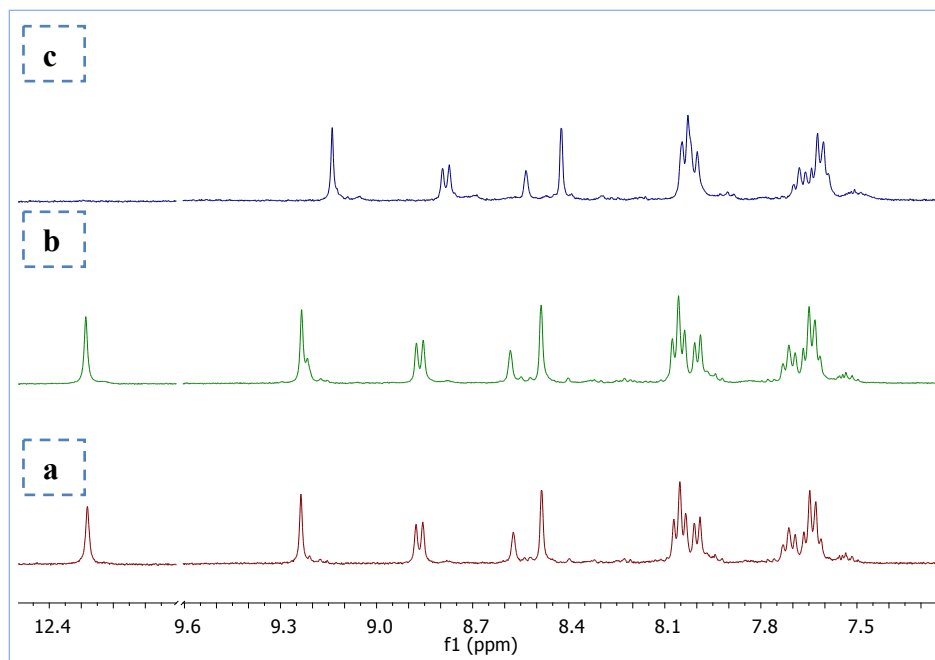


Figure S5. Partial ^1H NMR spectra of **L2** with addition of Al(III) a) 0 equiv b) 10.0 equiv c) After addition of excess D_2O in $\text{DMSO-}d_6$.

Acquisition Parameter

Source Type	ESI	Ion Polarity	Positive	Set Nebulizer	0.4 Bar
Focus	Not active	Set Capillary	4500 V	Set Dry Heater	180 °C
Scan Begin	50 m/z	Set End Plate Offset	-500 V	Set Dry Gas	4.0 l/min
Scan End	3000 m/z	Set Collision Cell RF	650.0 Vpp	Set Divert Valve	Waste

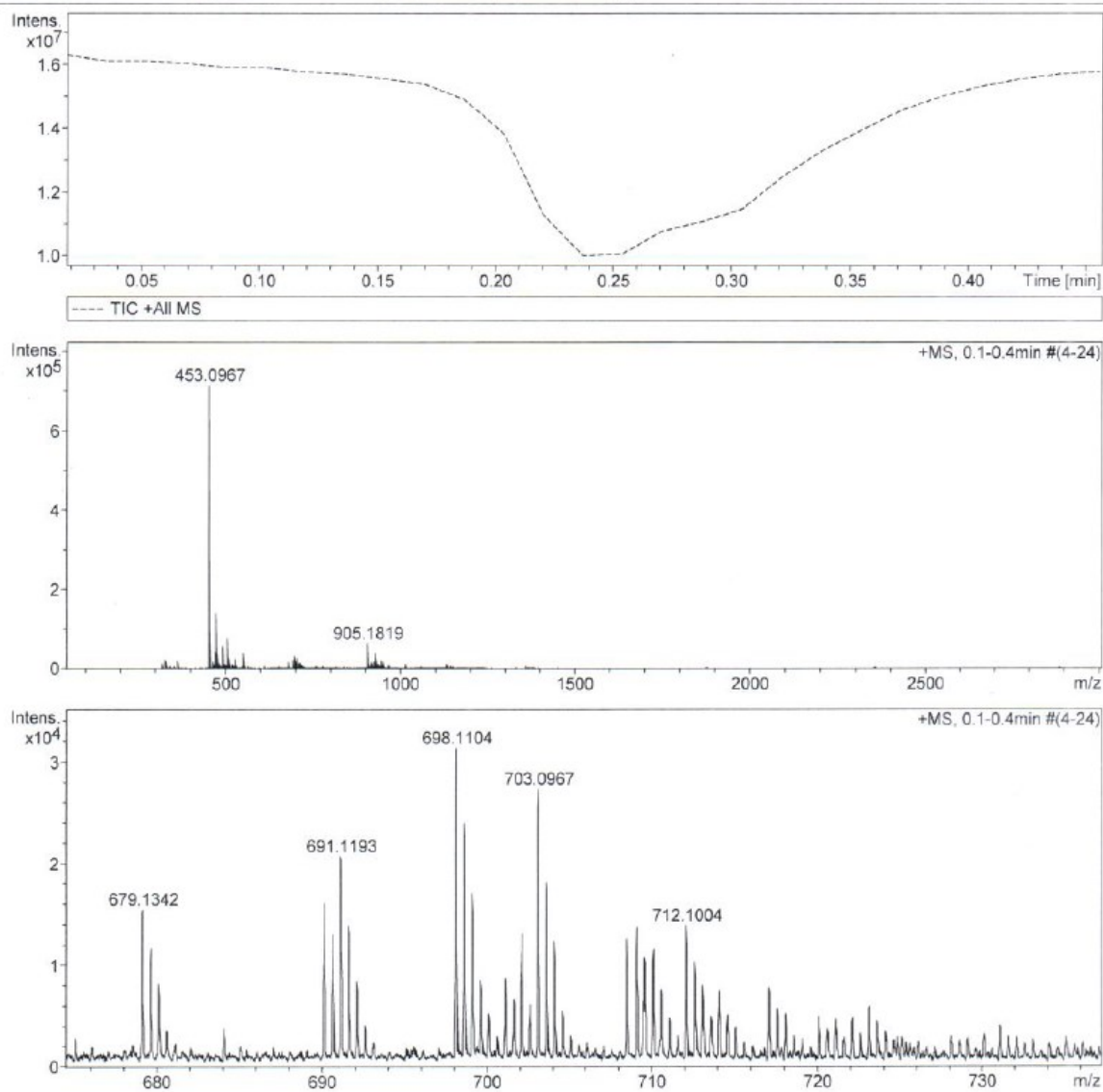


Figure S6. ESI-MS (HRMS) spectra of isolated Al(III) complex. The peak at 698.1104 is due to the (**L1** Na⁺ + Al(III) + 2H⁺ + 3NO₃⁻ + MeOH).

Analysis of complex. The interaction between receptor (**L1**) with Al(III) was also determined by LC-MS, FT-IR and NMR in solution as well as in isolated pure complex. **L1** was dissolved in water (10 mL) and an excess amount (5 fold) of the nitrated salt of Al(III) was added into the

solutions. The reaction mixtures were stirred at room temperature for 2 h and the solutions were analyzed by LC-MS instrument. The solvent was evaporated from the solution and IR analysis was performed using KBr plate. ^1H NMR was performed in $\text{DMSO-}d_6$. The change in proton signal has been recorded by adding 1-10 equiv Al(III) to the $\text{DMSO-}d_6$ solution of compound **L1**.

Fluorescence titration experiments were conducted to detect the F^- ion-induced fluorescence intensity changes of $[\text{L1} + \text{Al(III)}]$ complex, using KF as the F^- ion source. The emission peak at 436 nm gradually decreased upon addition of KF to the aqueous HEPES solution of the above optimized fluorescent $[\text{L1} + \text{Al(III)}]$ complex, and the fluorescence spectrum of the mixture was obtained at ambient temperature. The stoichiometric ratio of ligand (**L1**) and Al(III) was estimated to be 3:2 from Job's plot (Figure S7a).² The variation in fluorescence intensity **L1** (2×10^{-4} M) in presence of Al(III) (5.0 equiv) with pH ($\lambda_{\text{em}} \sim 436$ nm) is shown in Figure S7b.

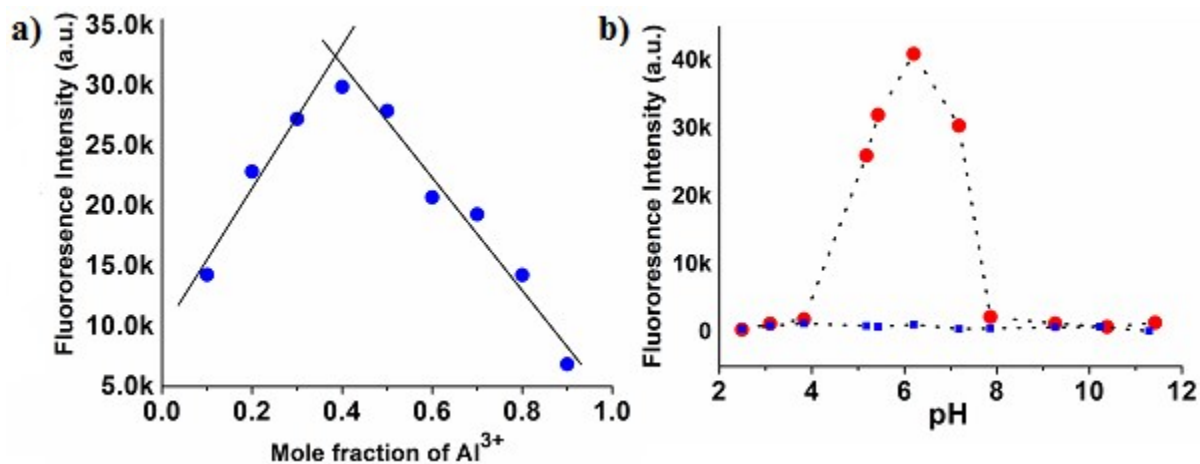


Figure S7. a) Job's plot for determining the stoichiometric complexation of **L1** with Al(III) in water. b) The variation in fluorescence intensity **L1** (2×10^{-4} M) in presence of Al(III) (5.0 equiv) with pH ($\lambda_{\text{em}} \sim 436$ nm).

Lowest detection limit of Al(III)

The LOD of Al(III) was calculated by following equation

$$\text{LOD} = K \cdot \sigma / s$$

Where $K=2$, σ is the standard deviation of blank measurement, s is the slope of intensity vs.

[Al(III)] plot

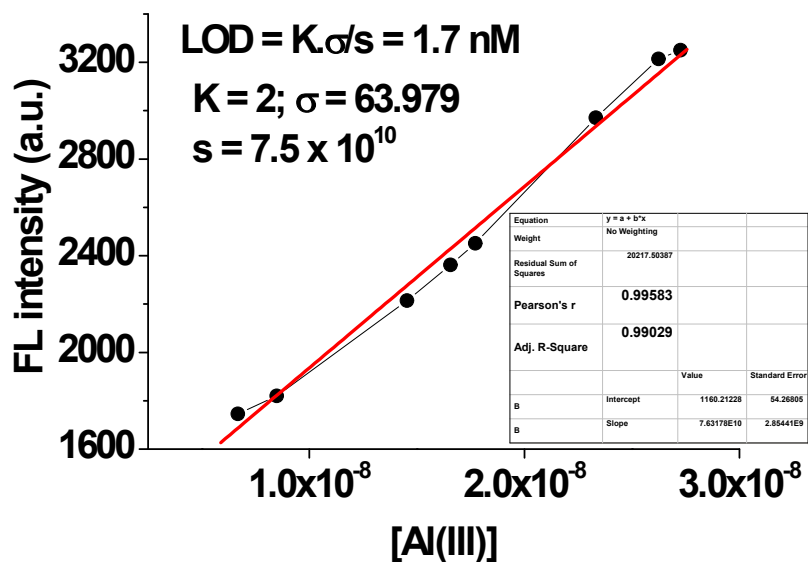


Figure S8. Calibration curve for lowest detection limit.

Here σ is found to be 63.97 and slope from the graph is 7.5×10^{10} . LOD calculated is 1.7nM.

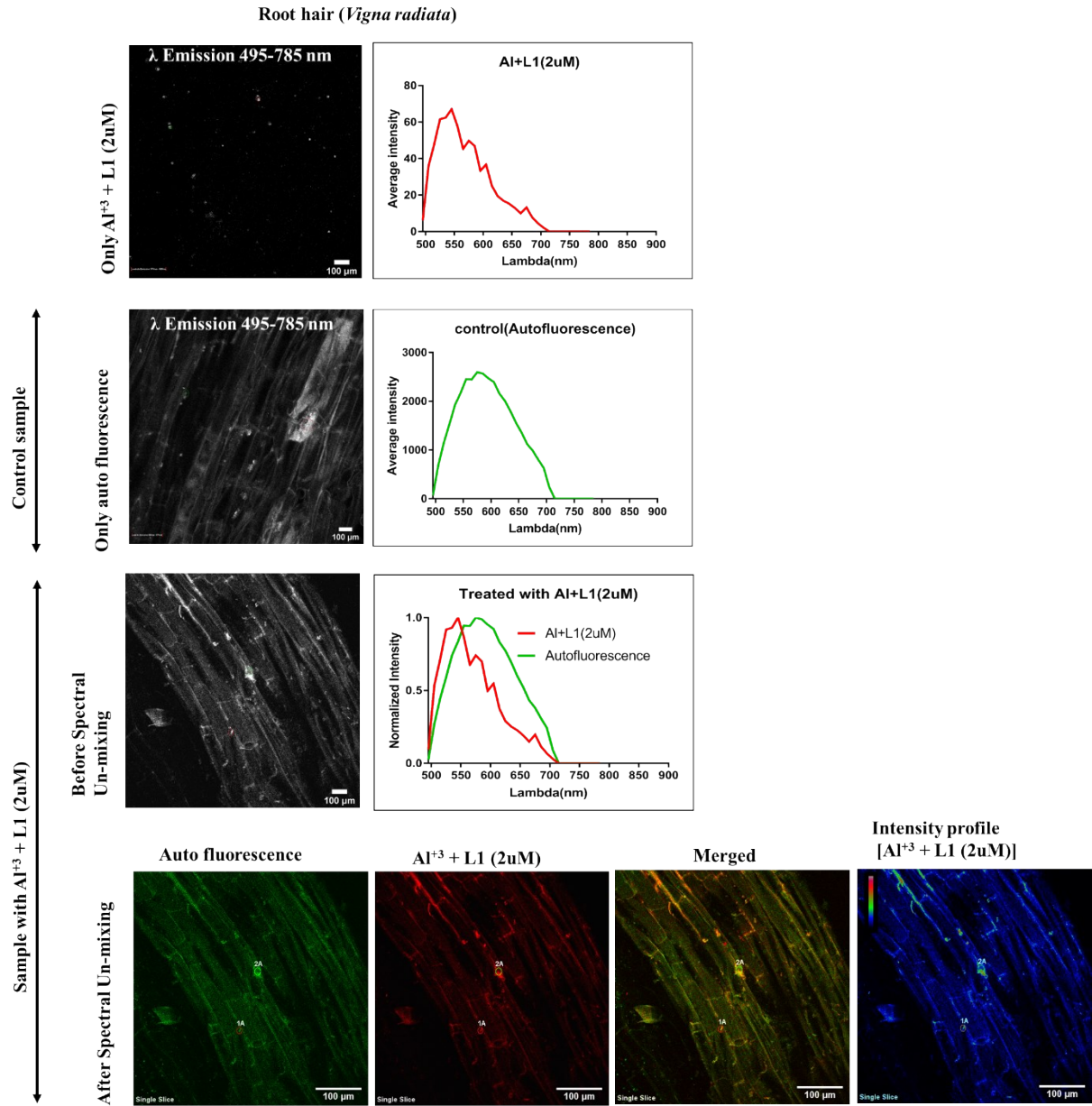


Figure S9. Comparative analysis of fluorescence (and auto-fluorescence) in control root hair cells and $[\text{Al}(\text{III}) + \text{L1}]$ -treated cells and extraction of **L1**-specific signals after spectral unmixing.

Table S1. Comparison Table of Lower Detection Limit (LOD) for Al(III) and F⁻ ion of L1 with other reported compounds.

Entry	LOD of Al(III)	LOD of F ⁻	Solvent	Method	Citation
1	1.7×10^{-9} M	2×10^{-12} M	Water	Fluorescence enhancement /quenching	<i>This Work</i>
2	0.092 μ M	0.112 μ M	Water	Fluorescence Quenching/ enhancement	<i>Sens. Actuators B: Chem.</i> 2016, 229, 138. ³
3	4.32 μ M	-	Water-methanol	Fluorescence enhancement	<i>Sens. Actuators B: Chem.</i> 2018, 260, 888. ⁴
4	30 μ M	-	THF-Tris-HCl	Fluorescence enhancement	<i>Sens. Actuators B: Chem.</i> 2018, 256, 276. ⁵
5	2 μ M	18 μ M	Water	Fluorescence	<i>ACS Appl. Mater. Interfaces</i> 2017, 9, 17359. ⁶
6	2.28 nM	0.13 μ M	Water (0.5% DMSO)	Fluorescence enhancement/ quenching	<i>Spectrochim. Acta A</i> 2019, 208, 131. ⁷
7	1.1×10^{-7} M	1.47 μ M	DMF/H ₂ O	Fluorescence enhancement/ quenching	<i>New J. Chem.</i> 2018, 42, 14978. ⁸
8	145 nM	-	Water	Fluorescence	<i>Analyst</i> 2018, 143, 5285. ⁹
9	0.7 μ M	-	Water-DMF	Fluorescence quenching	<i>J. Mat. Chem. A</i> 2017, 5, 13079. ¹⁰
10	-	1 \times nM	DMSO	Fluorescence enhancement	<i>J. Am. Chem. Soc.</i> 2010, 132, 17674-17677. ¹¹
11	-	5×10^{-5} M	THF	Ratiometric fluorescent	<i>ACS Appl. Nano Mater.</i> 2019, 2, 470-478. ¹²
12	-	0.10 ppm	Water	Ratiometric fluorescence	<i>ACS Appl. Mater. Interfaces</i> 2017, 9,

					18314. ¹³
13	-	50 μ M	Ethanol–water	Fluorescence quenching	<i>Sens. Actuators B: Chem.</i> 2010, 146, 260. ¹⁴
14	-	50 μ M	Water	Fluorescence enhanced	<i>Sens. Actuators B: Chem.</i> 2007, 125, 447. ¹⁵
15	-	12 ppb.	Ethanol–water	Fluorescence quenching	<i>Spectrochim. Acta A</i> 2006, 65, 565. ¹⁶
16	-	24 μ M	Water	Ratiometric fluorescent	<i>J. Mater. Chem. C</i> 2014, 2, 8599. ¹⁷
17	-	20 μ M	CH ₃ CN	Ratiometric fluorescent	<i>J. Mater. Chem.</i> 2012, 22, 5291. ¹⁸
18	-	1.5×10^{-5} M	Water	Fluorescence quenching	<i>Anal. Sci.</i> 2005, 21, 973. ¹⁹
19	-	5×10^{-6} M	Water	Fluorescence quenching	<i>Talanta</i> , 2006, 68, 1000. ²⁰
20	-	50 ppb	Water	Fluorescence enhancement	<i>Sci. Rep.</i> 2013 , 3, 2562. ²¹
21	5 μ M	-	DMSO	Fluorescence enhancement	<i>Inorg. Chem.</i> 2013 , 52, 7320. ²²
22	0.37 μ M	-	EtOH - H ₂ O	Fluorescence enhancement	<i>J. Lumin.</i> 2018 , 203, 113. ²³
23	1.09×10^{-9} M	-	Water	Fluorescence enhancement	<i>J. Photochem. Photobiol. A: Chem.</i> 2017 , 348, 246. ²
24	-	2.0 μ M	DCM	Ratiometric fluorescent	<i>Org. Lett.</i> , 2010 , 12, 3320. ²⁴
25	-	3.5×10^{-6} M	CHCl ₃	Fluorescence quenching	<i>Org. Lett.</i> , 2009 , 11, 5418. ²⁵

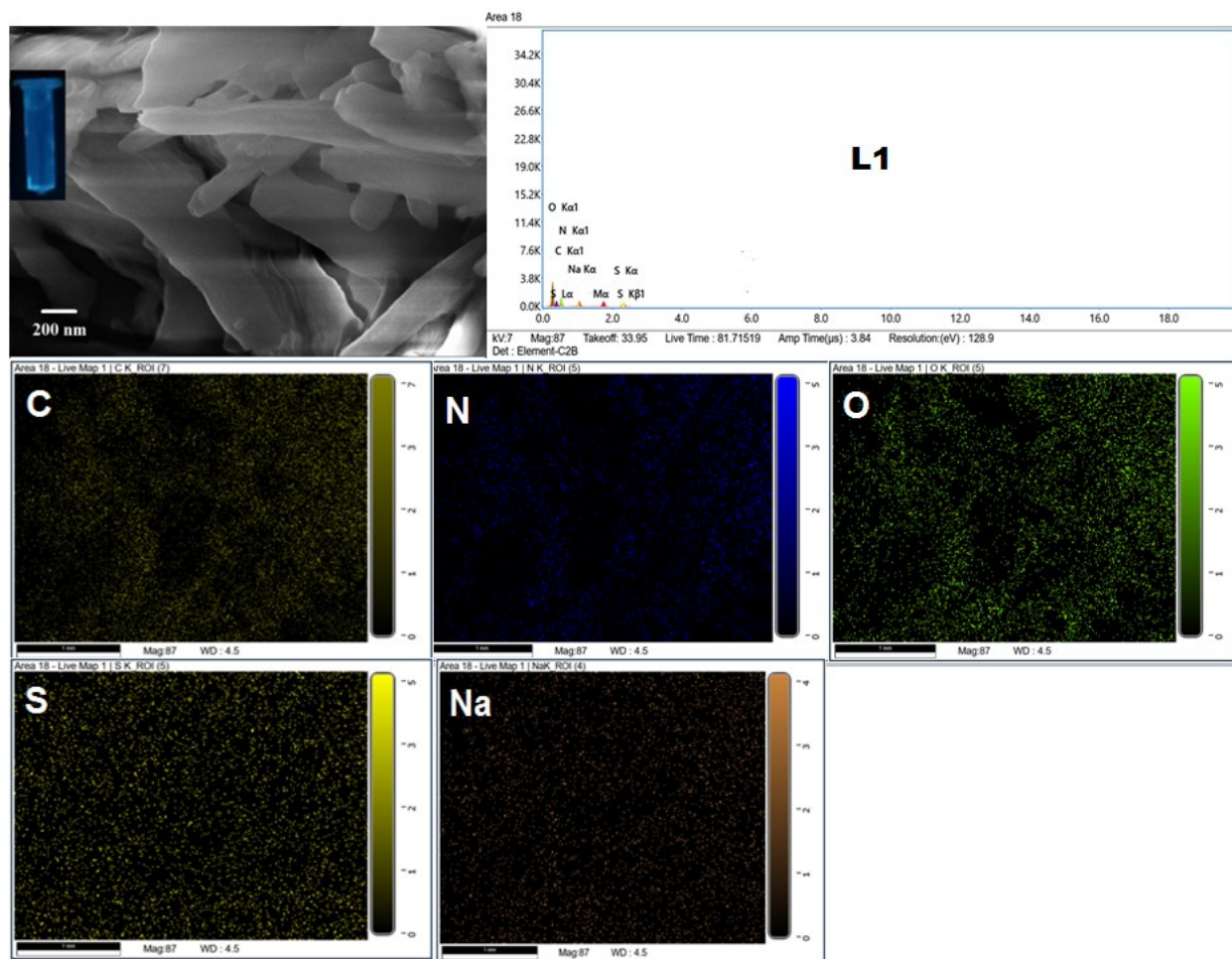


Figure S10.EDX and elemental mapping of L1.

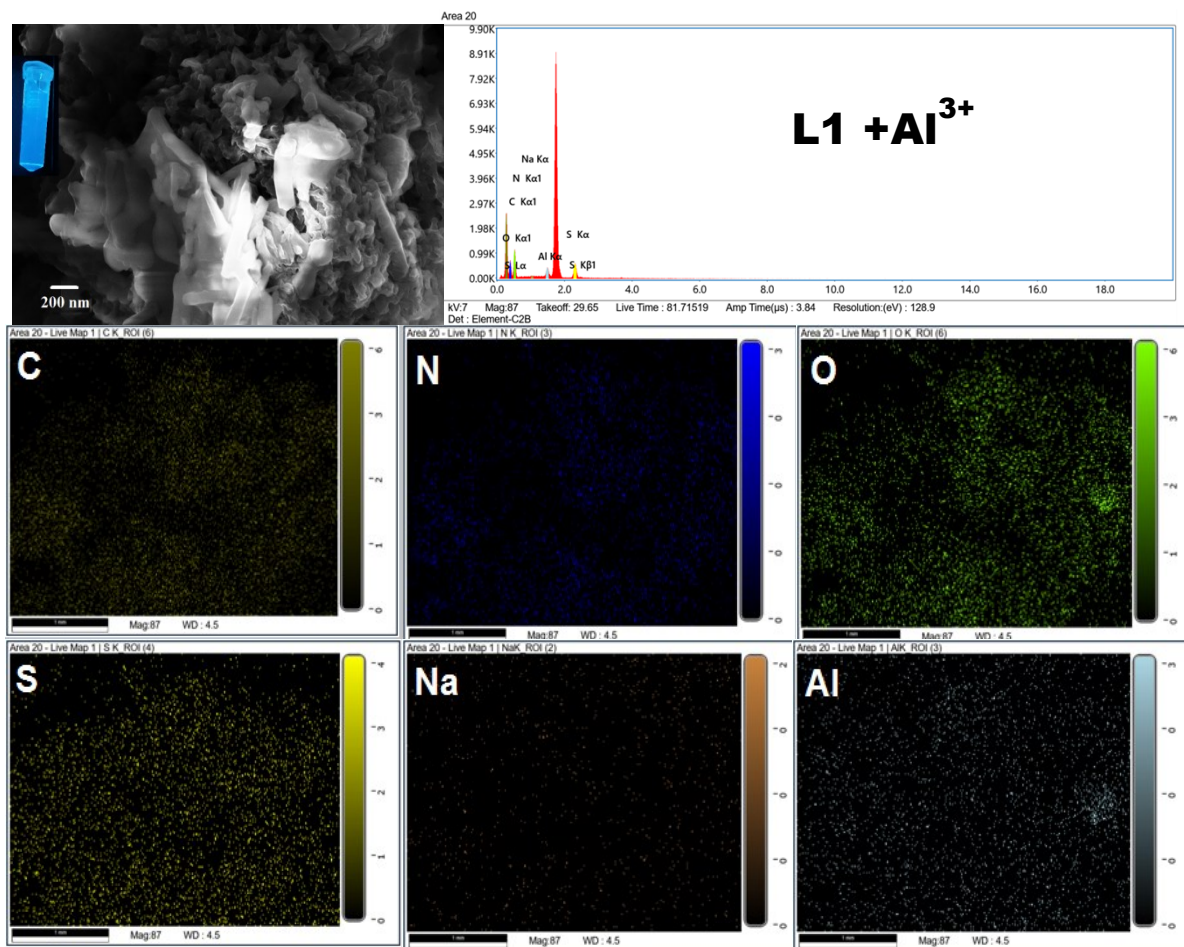


Figure S11.EDX and elemental mapping of [L1+ Al(III)] complex.

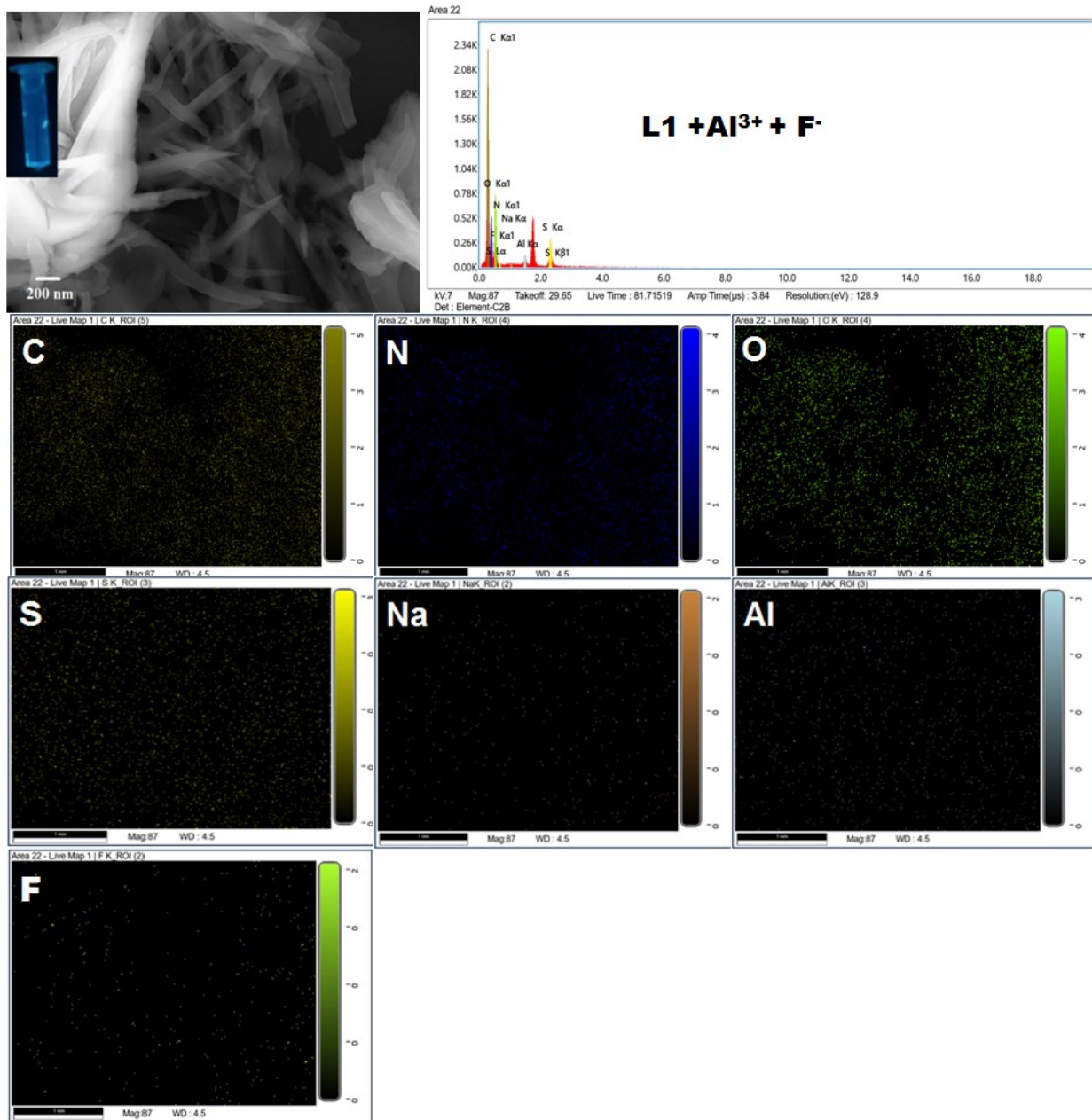


Figure S12.EDX and elemental mapping of [L1+ Al(III)] complex after addition of F⁻ ion.

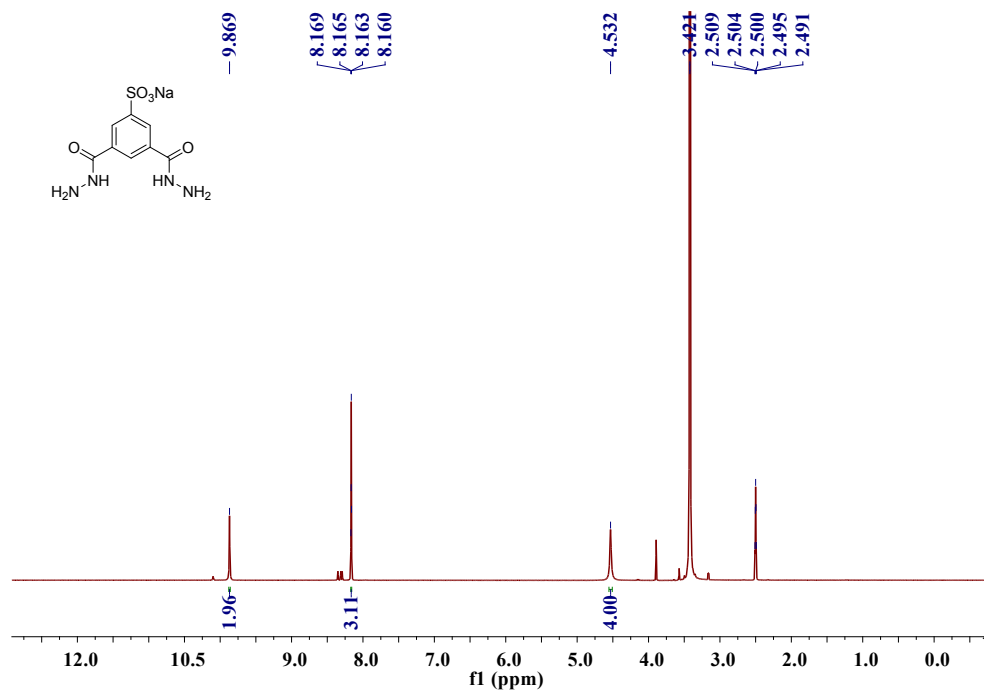


Figure S13. ^1H NMR spectrum of 1.

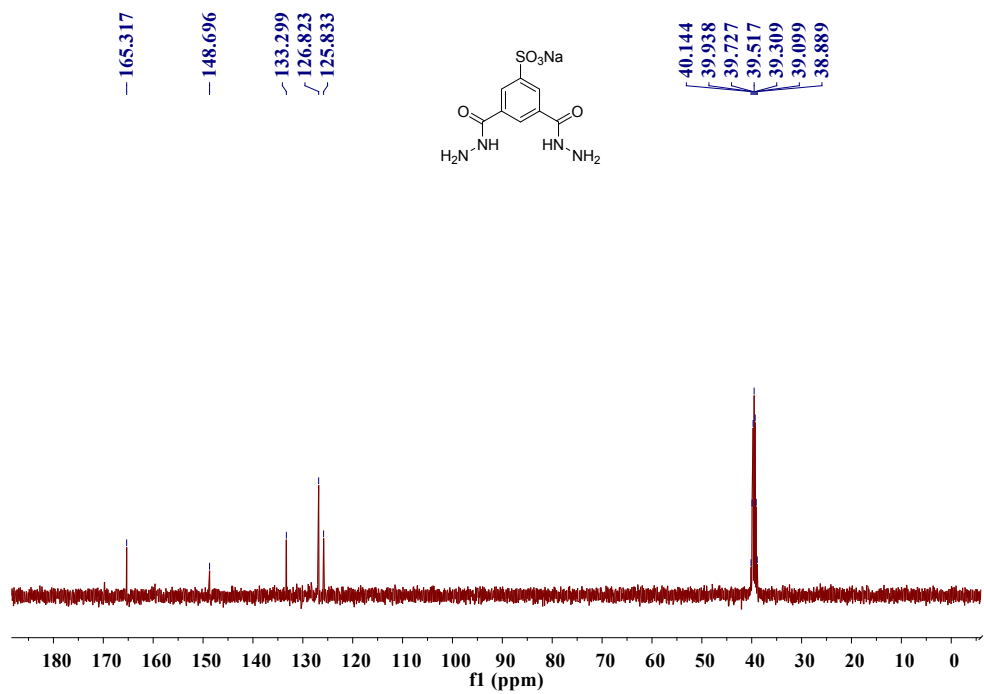


Figure S14. ^{13}C NMR spectrum of 1.

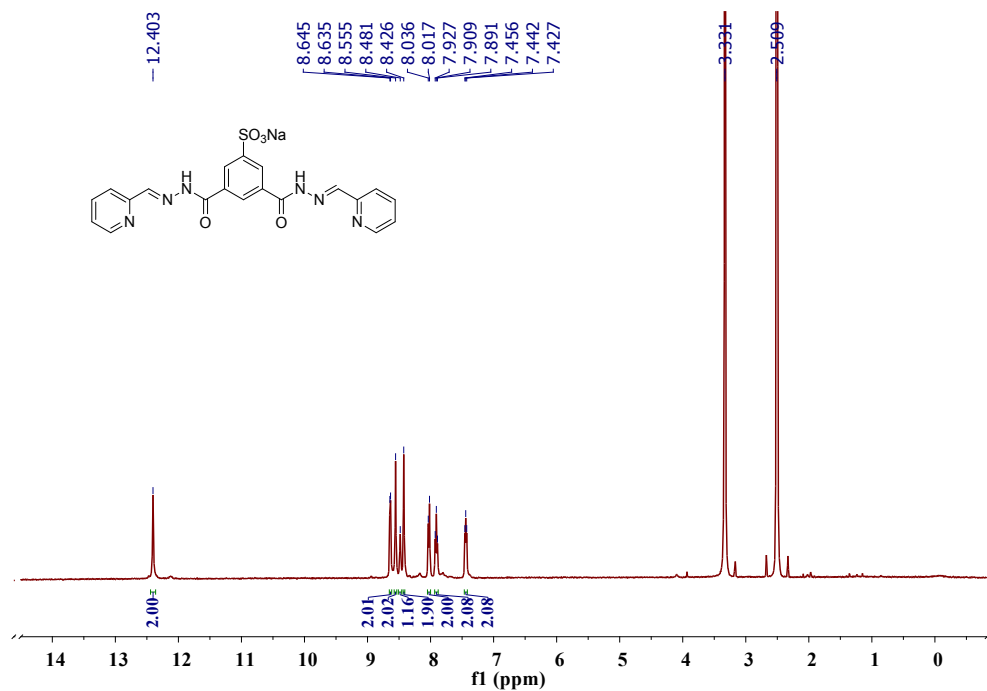


Figure S15. ¹H NMR spectrum of L1.

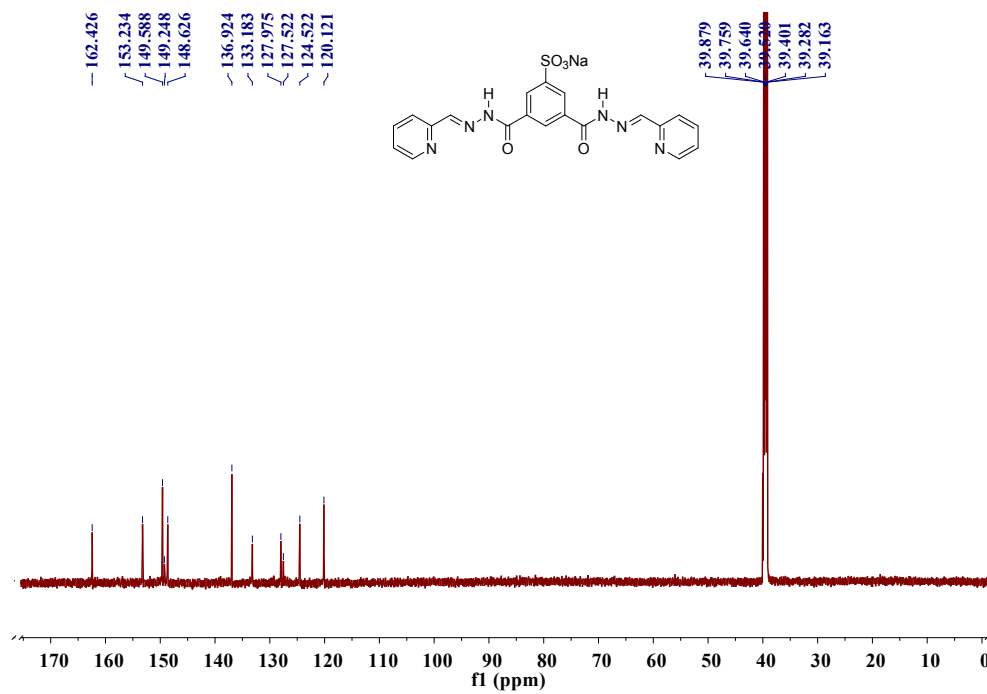


Figure S16. ¹³C NMR spectrum of L1.

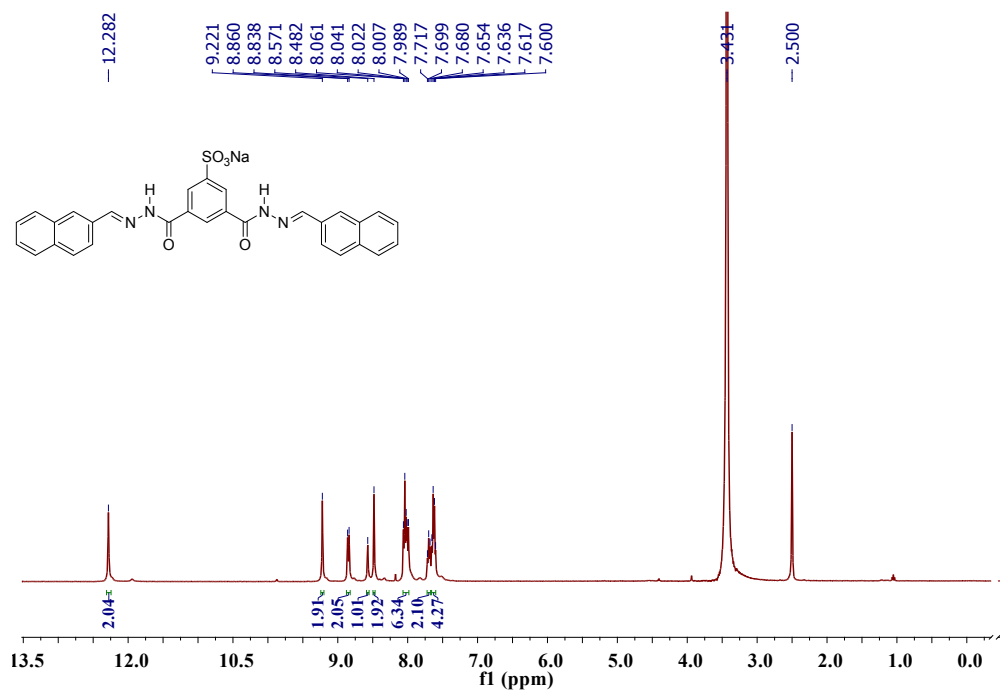


Figure S17. ¹H NMR spectrum of L2.

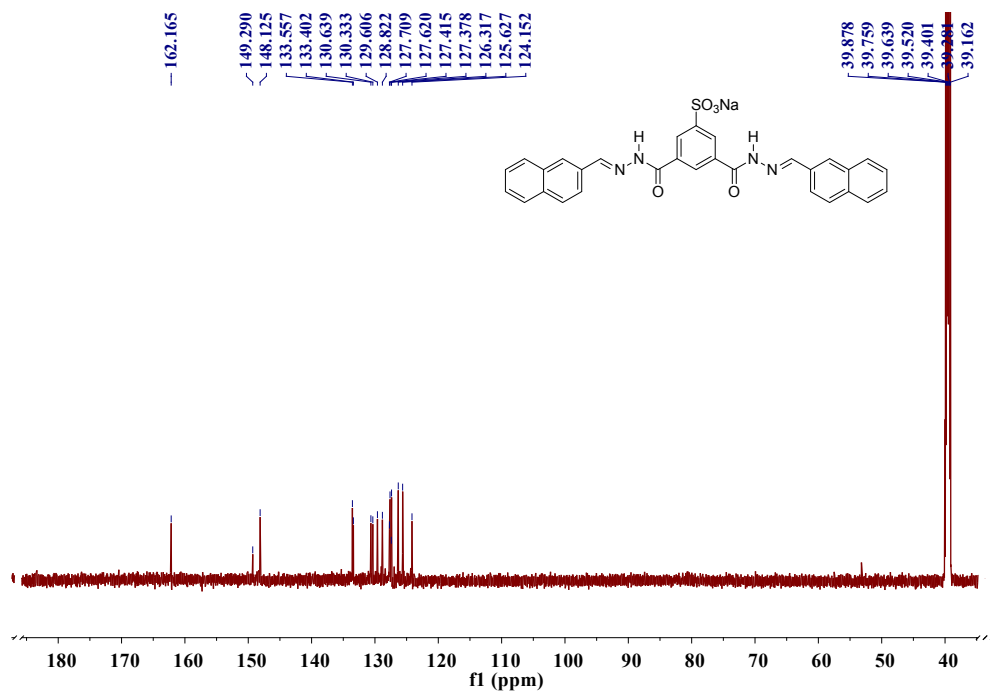


Figure S18. ¹³C NMR spectrum of L2.

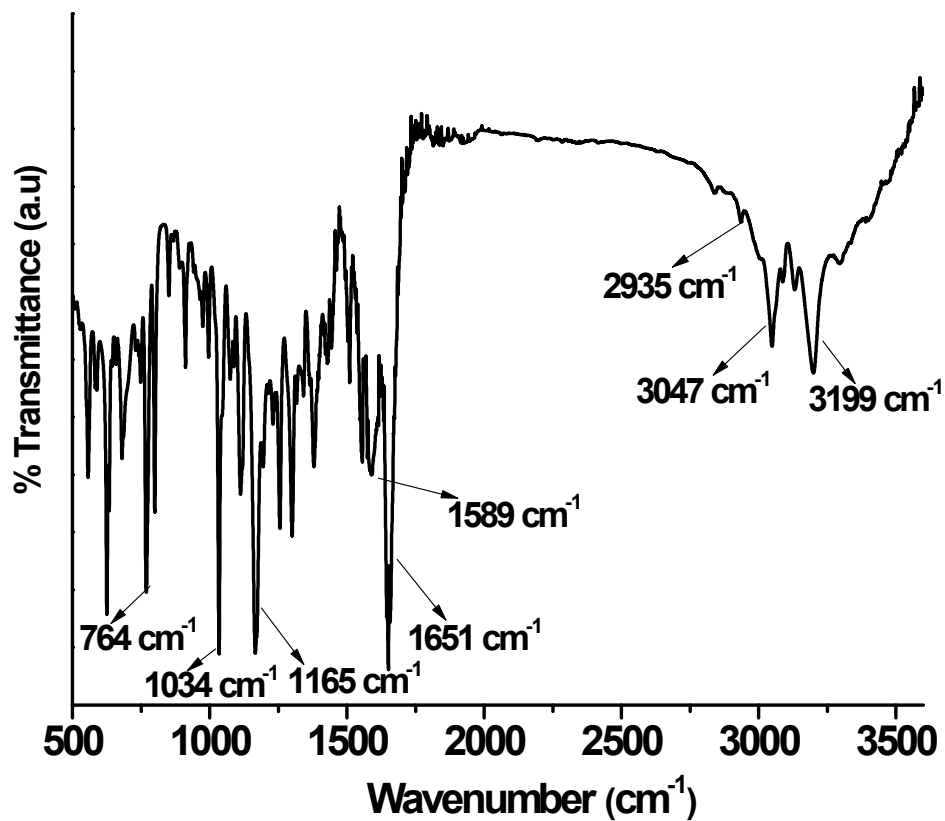


Figure S19. IR spectrum of L2.

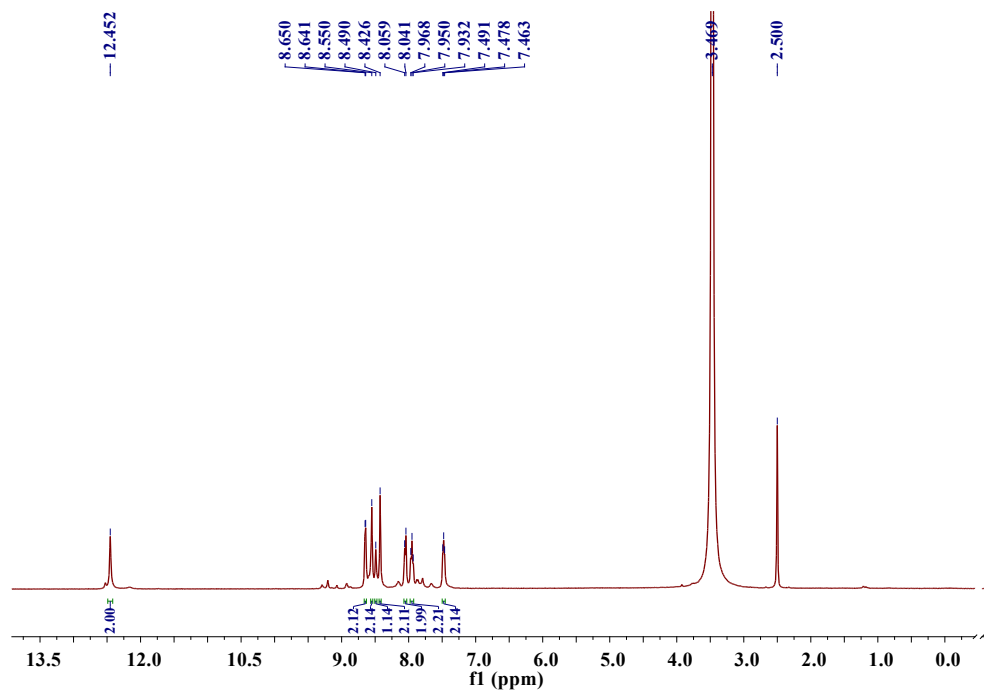


Figure S21. ^1H NMR of L1 with Al(III).

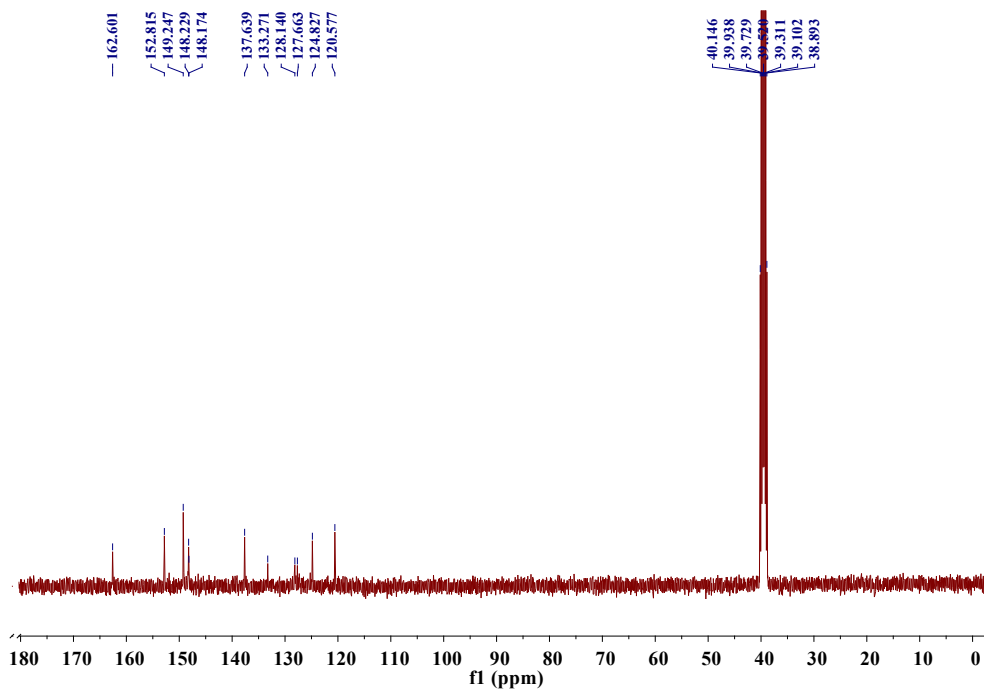


Figure S22. ^{13}C NMR of L1 with Al(III).

REFERENCES

1. A. C. Tedesco, D. M. Oliveira, Z. G. M. Lacava, R. B. Azevedo, E. C. D. Lima and P. C. Morais, *J. Magn. Magn. Mater.*, 2004, **272-276**, 2404-2405.
2. S. R. Gupta, P. Singh, B. Koch and V. P. Singh, *J. Photochem. Photobiol. A: Chem.*, 2017, **348**, 246-254.
3. Q. Diao, P. Ma, L. Lv, T. Li, Y. Sun, X. Wang and D. Song, *Sens. Actuators B: Chem.*, 2016, **229**, 138-144.
4. M. Kumar, A. Kumar, M. S. H. Faizi, S. Kumar, M. K. Singh, S. K. Sahu, S. Kishor and R. P. John, *Sens. Actuators B: Chem.*, 2018, **260**, 888-899.
5. D. Yao, X. Huang, F. Guo and P. Xie, *Sens. Actuators B: Chem.*, 2018, **256**, 276-281.
6. A. Kumar, M. Bhatt, G. Vyas, S. Bhatt and P. Paul, *ACS Appl. Mater. Interfaces*, 2017, **9**, 17359-17368.
7. X.-y. Kong, L.-J. Hou, X.-q. Shao, S.-M. Shuang, Y. Wang and C. Dong, *Spectrochim. Acta A*, 2019, **208**, 131-139.
8. Y.-P. Wu, F.-U. Rahman, M. Z. Bhatti, S.-B. Yu, B. Yang, H. Wang, Z.-T. Li and D.-W. Zhang, *New J. Chem.*, 2018, **42**, 14978-14985.
9. L. N. Neupane, P. K. Mehta, S. Oh, S.-H. Park and K.-H. Lee, *Analyst*, 2018, **143**, 5285-5294.
10. W.-M. Chen, X.-L. Meng, G.-L. Zhuang, Z. Wang, M. Kurmoo, Q.-Q. Zhao, X.-P. Wang, B. Shan, C.-H. Tung and D. Sun, *J. Mat. Chem. A*, 2017, **5**, 13079-13085.
11. S. Guha and S. Saha, *J. Am. Chem. Soc.*, 2010, **132**, 17674-17677.
12. H. Zhou, M. H. Chua, H. R. Tan, T. T. Lin, B. Z. Tang and J. Xu, *ACS Appl. Nano Mater.*, 2019, **2**, 470-478.

13. Y. Liu, Q. Ouyang, H. Li, Z. Zhang and Q. Chen, *ACS Appl. Mater. Interfaces*, 2017, **9**, 18314-18321.
14. F. Wang, J. Wu, X. Zhuang, W. Zhang, W. Liu, P. Wang and S. Wu, *Sens. Actuators B: Chem.*, 2010, **146**, 260-265.
15. J.-S. Wu, F. Wang, W.-M. Liu, P.-F. Wang, S.-K. Wu, X. Wu and X.-H. Zhang, *Sens. Actuators B: Chem.*, 2007, **125**, 447-452.
16. R. S. Sathish, U. Sujith, G. N. Rao and C. Janardhana, *Spectrochim. Acta A*, 2006, **65**, 565-570.
17. K. Dhanunjayarao, V. Mukundam and K. Venkatasubbaiah, *J. Mater. Chem. C*, 2014, **2**, 8599-8606.
18. Y. Bao, B. Liu, F. Du, J. Tian, H. Wang and R. Bai, *J. Mater. Chem.*, 2012, **22**, 5291-5294.
19. T. Balaji and H. Matsunaga, *Anal. Sci.*, 2005, **21**, 973-977.
20. H. Matsunaga, C. Kanno, H. Yamada, Y. Takahashi and T. M. Suzuki, *Talanta*, 2006, **68**, 1000-1004.
21. F. M. Hinterholzinger, B. Rühle, S. Wuttke, K. Karaghiosoff and T. Bein, *Sci. Rep.*, 2013, **3**, 2562.
22. W.-H. Ding, W. Cao, X.-J. Zheng, D.-C. Fang, W.-T. Wong and L.-P. Jin, *Inorg. Chem.*, 2013, **52**, 7320-7322.
23. Q. Wang, H. Sun, L. Jin, W. Wang, Z. Zhang and Y. Chen, *J. Lumin.*, 2018, **203**, 113-120.
24. Y. Qu, J. Hua and H. Tian, *Org. Lett.*, 2010, **12**, 3320-3323.

25. S. V. Bhosale, S. V. Bhosale, M. B. Kalyankar and S. J. Langford, *Org. Lett.*, 2009, **11**, 5418-5421.